Near-field radiative heat transfer and van der Waals friction between closely spaced graphene and amorphous SiO_2

A.I.Volokitin[1,2*] and B.N.J.Persson[1]
[1] *Institut für Festkörperforschung, Forschungszentrum Jülich, D-52425, Germany and*
[2] *Samara State Technical University, 443100 Samara, Russia*

We study the radiative heat transfer and the van der Waals friction between graphene and an amorphous SiO_2 substrate. We study the surface phonon-polaritons contribution to the low-field mobility as a function of temperature and of carrier density. We find that the electric current saturate at a high electric field, in agreement with experiment. The saturation current depends weakly on the temperature, which we attribute to the "quantum" friction between the graphene carriers and the substrate optical phonons. We calculate the frictional drag between two graphene sheets caused by van der Waals friction, and find that this drag can induce a high enough voltage which can be easily measured experimentally. We find that for nonsuspended graphene the near-field radiative heat transfer, and the heat transfer due to direct phononic coupling, are of the same order of magnitude at low electric field. The phononic contribution to the heat transfer dominates at high field. For large separation between graphene and the substrate the heat transfer is dominated by the near-field radiative heat transfer.

PACS: 47.61.-k, 44.40.+a, 68.35.Af

Introduction. Graphene, the recently isolated single-layer carbon sheet, consist of carbon atoms closely packed in a flat two-dimensional crystal lattice. The unique electronic and mechanical properties of graphene[1,2] is being actively explored both theoretically and experimentally because of its importance for fundamental physics, and for possible technological applications[3]. In particular, a great deal of attention has been devoted to the applications of graphene for electronics and sensoring[1,3].

Graphene, as for all media, is surrounded by a fluctuating electromagnetic field due to the thermal and quantum fluctuations of the current density. Outside the bodies this fluctuating electromagnetic field exists partly in the form of propagating electromagnetic waves and partly in the form of evanescent waves. The theory of the fluctuating electromagnetic field was developed by Rytov[4–6]. A great variety of phenomena such as Casimir-Lifshitz forces[7], near-field radiative heat transfer[8], non-contact friction[9–12], and the frictional drag in low-dimensional systems[13,14], can be described using this theory.

In the present paper we apply the theories of the near-field radiative heat transfer and the van der Waals friction to study the electric transport properties, and the heat generation and dissipation in graphene, mediated by the fluctuating electromagnetic field. The charge carriers in graphene absorbed on, or located close to, a substrate experience a friction due to interaction with substrate. This friction affects the graphene carrier mobility and leads to the heat generation. The existing microscopic theories[15,16] involve several fitting parameters, while our theory is macroscopic. In this theory the electromagnetic interaction between graphene and a substrate is described by the dielectric functions of the materials which can be accurately determined from experiment.

The development of more powerful microelectronic devices results in increasing dissipated power (per unit volume), and developing structures with smaller heat production and better cooling strategies, is one of the "grand challenge" of modern electronics[17]. The heat generated in microelectronic devices leads to elevated device operation temperatures, performance reduction, and ultimately to hardware failures. The three classical mechanisms of heat transfer are convection, conduction, and radiation. The former is not important in existing circuit architecture having no fluid or gas flowing inside.

Graphene interact very weakly with most substrates mainly via van der Waals forces. According to theoretical calculations[18] the thermal contact conductance due to the direct phononic coupling for the interface between graphene and a perfectly smooth (amorphous) SiO_2 substrate is $\alpha_{\rm ph} \approx 3 \times 10^8 {\rm Wm}^{-2}{\rm K}^{-1}$, and according to experiment[19] (at room temperature) the thermal contact conductance ranges from $8{\times}10^7$ to $1.7{\times}10^8 {\rm Wm}^{-2}{\rm K}^{-1}$ (however, these values are probably influenced by the substrate surface roughness).

At large separation $d \gg \lambda_T = k_B T/\hbar$ the radiative heat transfer is determined by the Stefan-Boltzman law, according to which $\alpha = 4\sigma T^3$. In this limiting case the heat transfer between two bodies is determined by the propagating electromagnetic waves radiated by the bodies, and does not depend on the separation d. At $T = 300$K this law predicts the (very small) thermal contact conductance, $\alpha \approx 6$ ${\rm Wm}^{-2}{\rm K}^{-1}$. However, as was first predicted

* Corresponding author. *E-mail address*:alevolokitin@yandex.ru

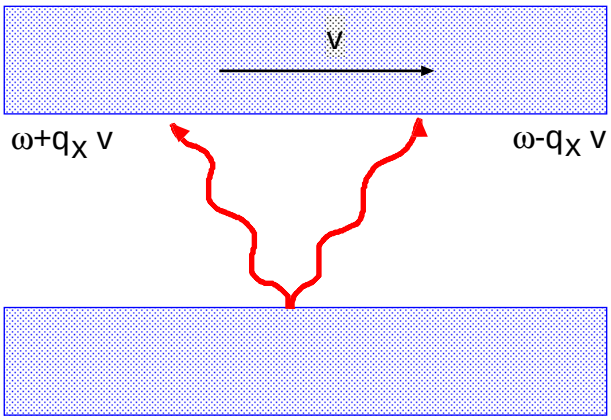

FIG. 1: Two bodies moving relative to each other will experience van der Waals friction due to Doppler shift of the electromagnetic waves emitted by them.

theoretically[8], and recently confirmed experimentally[20,21], at short separation $d \ll \lambda_T$, the heat transfer may increase by many orders of magnitude due to the evanescent electromagnetic waves; this is often referred to as photon tunneling. Particularly strong enhancement occurs if the surfaces of the bodies can support localized surface modes such as surface plasmon-polaritons, surface phonon-polaritons, or adsorbate vibrational modes[10,22]. In two recent experiments[20,21] the thermal contact conductance between a silica plate and a silica sphere was measured from 30 nm separation out to few micrometers. Heat transfer across the plate-sphere gap causes the cantilever to bent very slightly, and this was measured by optical fiber interferometry.

The theory of the radiative heat transfer developed in Ref.[8] is only valid for bodies at rest. A more general theory of the radiative heat transfer between moving bodies, with arbitrary relative velocities, was developed in Ref.[12]. This theory can be applied to calculate the radiative heat transfer between carriers (moving with the drift velocity v) in graphene and the substrate. According to theory[10], for the graphene-SiO_2 interface the maximum of the contribution of the radiative heat transfer to the thermal contact conductivity is $\alpha_{max} \sim (k_B T)^2 n/\hbar$, where n is the concentration of carriers in graphene. At room temperature and $n \approx 10^{13}\text{cm}^{-2}$ this gives $\alpha_{max} \sim 10^7 \text{Wm}^{-2}\text{K}^{-1}$. However this estimation does not take into account that the charge carriers in graphene are moving relative to the substrate. Relative motion of charge carriers in graphene corresponds to an effective increase in the temperature difference between graphene and substrate, what leads to an increase in thermal contact conductance. Thus, for nonsuspended graphene the thermal contact conductivity due to near-field radiative heat transfer, and due to direct phononic mechanism, can be of the same order. However for suspended graphene, the main contribution results from radiative heat transfer since this process exhibit a much weaker distance dependence than for the phononic contribution.

The radiative heat transfer is closely connected with the van der Waals friction. This friction is due to the Doppler effect. Assume that a graphene sheet is separated from the substrate by a sufficiently wide insulator gap, which prevents particles from tunneling across it. If the charge carriers inside graphene move with velocity v relative to the substrate, a frictional stress will act on them. This frictional stress is related to an asymmetry of the reflection amplitude along the direction of motion; see Fig. 1. If the substrate emits radiation, then in the rest reference frame of charge carriers in graphene these waves are Doppler shifted which will result in different reflection amplitudes. The same is true for radiation emitted by moving charge carriers in graphene. The exchange of "Doppler-shifted-photons" will result in momentum transfer between graphene and substrate, which is the origin of the van der Waals friction.

Theory. Let us consider graphene and a substrate with flat parallel surfaces at separation $d \ll \lambda_T = c\hbar/k_B T$. Assume that the free charge carriers in graphene move with the velocity $v \ll c$ (c is the light velocity) relative to other medium. According to Ref.[9–12] the frictional stress F_x acting on charge carriers in graphene, and the radiative heat flux S_z across the surface of substrate, both mediated by a fluctuating electromagnetic field, are determined by

$$F_x = \frac{\hbar}{\pi^3}\int_0^\infty dq_y \int_0^\infty dq_x q_x e^{-2qd}\Bigg\{\int_0^\infty d\omega\Bigg(\frac{\text{Im}R_d(\omega)\text{Im}R_g(\omega^+)}{\mid 1-e^{-2qd}R_d(\omega)R_g(\omega^+)\mid^2}\times$$

$$[n_d(\omega)-n_g(\omega^+)] + \frac{\text{Im}R_d(\omega^+)\text{Im}R_g(\omega)}{\mid 1-e^{-2qd}R_d(\omega^+)R_g(\omega)\mid^2}[n_g(\omega)-n_d(\omega^+)]\Bigg)+$$

$$\int_0^{q_x v} d\omega \frac{\mathrm{Im}R_d(\omega)\mathrm{Im}R_g(\omega^-)}{\mid 1-e^{-2qd}R_d(\omega)R_g(\omega^-)\mid^2}[n_g(\omega^-)-n_d(\omega)]\Bigg\}, \tag{1}$$

$$S_z=\frac{\hbar}{\pi^3}\int_0^\infty dq_y\int_0^\infty dq_x e^{-2qd}\Bigg\{\int_0^\infty d\omega\Bigg(-\frac{\omega\mathrm{Im}R_d(\omega)\mathrm{Im}R_g(\omega^+)}{\mid 1-e^{-2qd}R_d(\omega)R_g(\omega^+)\mid^2}\times$$

$$[n_d(\omega)-n_g(\omega^+)]+\frac{\omega^+\mathrm{Im}R_d(\omega^+)\mathrm{Im}R_g(\omega^)}{\mid 1-e^{-2qd}R_d(\omega^+)R_g(\omega)\mid^2}[n_g(\omega)-n_d(\omega^+)]\Bigg)+$$

$$\int_0^{q_x v} d\omega \frac{\omega\mathrm{Im}R_d(\omega)\mathrm{Im}R_g(\omega^-)}{\mid 1-e^{-2qd}R_d(\omega)R_g(\omega^-)\mid^2}[n_g(\omega^-)-n_d(\omega)]\Bigg\}, \tag{2}$$

where $n_i(\omega)=[\exp(\hbar\omega/k_BT_i-1]^{-1}$ $(i=g,d)$, $T_{g(d)}$ is the temperature of graphene (substrate), R_i is the reflection amplitude for surface i for p -polarized electromagnetic waves, and $\omega^\pm=\omega\pm q_xv$. The reflection amplitude for graphene (substrate) is determined by[13]

$$R_{g(d)}=\frac{\epsilon_{g(d)}-1}{\epsilon_{g(d)}+1}, \tag{3}$$

where $\epsilon_{g(d)}$ is the dielectric function for graphene (substrate).

In the study below we used the dielectric function of graphene, which was calculated recently within the random-phase approximation (RPA)[23,24]. The small (and constant) value of the graphene Wigner-Seitz radius r_s indicates that it is a weakly interacting system for all carries densities, making the RPA an excellent approximation for graphene (RPA is asymptotically exact in the $r_s\ll 1$ limit). The dielectric function is an analytical function in the upper half-space of the complex ω-plane:

$$\epsilon_g(\omega,q)=1+\frac{4k_Fe^2}{\hbar v_Fq}-\frac{e^2q}{2\hbar\sqrt{\omega^2-v_F^2q^2}}\Bigg\{G\Bigg(\frac{\omega+2v_Fk_F}{v_Fq}\Bigg)-G\Bigg(\frac{\omega-2v_Fk_F}{v_Fq}\Bigg)-i\pi\Bigg\}, \tag{4}$$

where

$$G(x)=x\sqrt{1-x^2}-\ln(x+\sqrt{1-x^2}), \tag{5}$$

where the Fermi wave vector $k_F=(\pi n)^{1/2}$, n is the concentration of charge carriers, the Fermi energy $\epsilon_F=\gamma k_F=\hbar v_Fk_F$, $\gamma=\hbar v_F\approx 6.5$ eVÅ, and v_F is the Fermi velocity.

The dielectric function of amorphous SiO_2 can be described using an oscillator model[25]

$$\epsilon(\omega)=\epsilon_\infty+\sum_{j=1}^{2}\frac{\sigma_j}{\omega_{0,j}^2-\omega^2-i\omega\gamma_j}, \tag{6}$$

where parameters $\omega_{0,j}$, γ_j and σ_j were obtained by fitting the actual ϵ for SiO_2 to the above equation, and are given by $\epsilon_\infty=2.0014$, $\sigma_1=4.4767\times 10^{27}\mathrm{s}^{-2}$, $\omega_{0,1}=8.6732\times 10^{13}\mathrm{s}^{-1}$, $\gamma_1=3.3026\times 10^{12}\mathrm{s}^{-1}$, $\sigma_2=2.3584\times 10^{28}\mathrm{s}^{-2}$, $\omega_{0,2}=2.0219\times 10^{14}\mathrm{s}^{-1}$, and $\gamma_1=8.3983\times 10^{12}\mathrm{s}^{-1}$.

The equilibrium or steady state temperature can be obtained from the condition that the heat power generated by friction must be equal to the heat transfer across the substrate surface

$$F_x(T_d,T_g)v=S_z(T_d,T_g)+\alpha_{ph}(T_g-T_d), \tag{7}$$

where the second term in Eq. (7) takes into account the heat transfer through direct phononic coupling; α_{ph} is the thermal contact conductance due to phononic coupling.

Results. At small velocities ($v\ll v_F$) the friction force depends linearly on v: $F_x=\Gamma v$, where the friction coefficient Γ is determined by

$$\Gamma=\frac{\hbar}{2\pi^2}\int_0^\infty d\omega\Bigg(-\frac{\partial n_d(\omega)}{\partial\omega}\Bigg)\int_0^\infty dqq^3e^{-2qd}\frac{\mathrm{Im}R_d(\omega)\mathrm{Im}R_g(\omega)}{\mid 1-e^{-2qd}R_d(\omega)R_g(\omega)\mid^2} \tag{8}$$

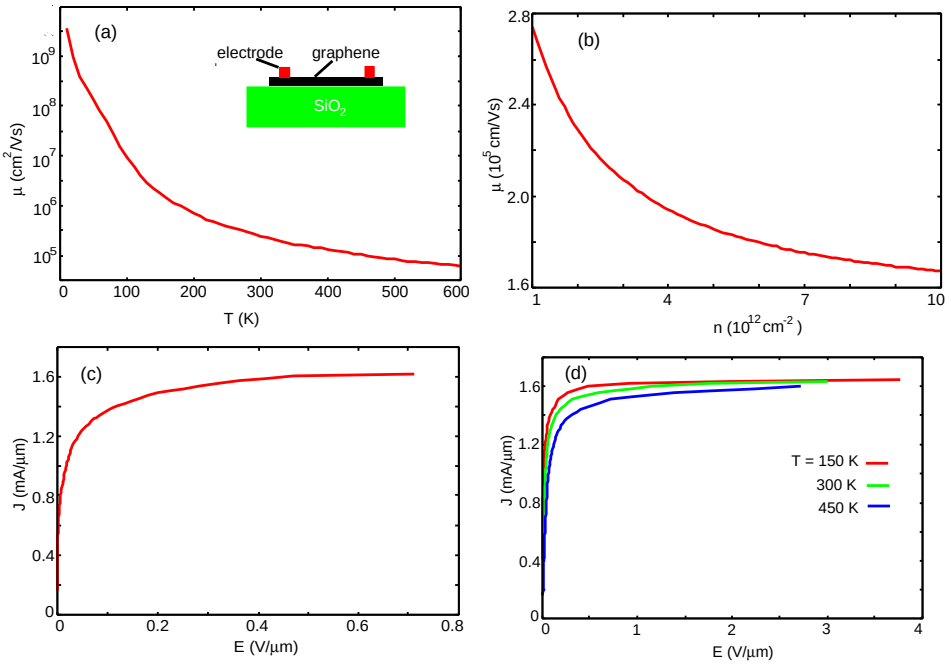

FIG. 2: The role of the interaction between phonon polaritons in SiO_2 and free carriers in graphene for graphene field-effect transistor transport. The separation between graphene and SiO_2 is $d = 3.5$Å. (a) Dependence of the low-field mobility on the temperature. Concentration of charge carriers $n = 10^{12}\text{cm}^{-12}$. (b) Dependence of the low-field mobility on the concentration of charge carriers n for $T_d = T_g = 300$ K. (c) Current density-electric field dependence at $T = 0$ K, $n = 10^{12}\text{cm}^{-12}$. (d) The same as in (c) but for different temperatures.

The low-field mobility can be described using Matthiessen's rule

$$\mu^{-1} = \mu_{int}^{-1} + \mu_{ext}^{-1}, \tag{9}$$

where μ_{int} is the intrinsic mobility due to scattering of the graphene free carriers against the acoustic and optical phonons in graphene, and μ_{ext} is the extrinsic mobility due to scattering against the optical phonons in the substrate. According to the theory of the van der Waals friction $\mu_{ext} = ne/\Gamma$. Scattering of the graphene carriers by the acoustic phonons of graphene places an intrinsic limits on the low-field room temperature mobility given by $\mu = 200000\text{cm}^2/\text{Vs}$ at the carriers density 10^{12}cm^{-2} [26]. However, for graphene on SiO_2 the mobility of the graphene carriers is reduced to $\mu = 40000\text{cm}^2/\text{Vs}$. This reduction must result partly from interface imperfections, and partly from scattering of the graphene carriers from the optical phonons of the SiO_2 substrate.

Fig. 2a shows the calculated dependence of the low-field mobility on the temperature, due to scattering from the optical phonons in SiO_2. The calculations were performed using the theory of the van der Waals friction. The mobility is characterized by a strong temperature dependence. At room temperature the calculated mobility $\mu \approx 3 \times 10^5$ cm^2/Vs, which is approximately one order of magnitude larger than the mobility calculated in Ref.[16]. This indicates that for graphene adsorbed on SiO_2 the main contribution to the low-field mobility comes not from scattering from the optical phonons in SiO_2, but from scattering from point defects on the interface.

Fig. 2b shows the dependence of the mobility at $T_d = 300$ K on the charge density n. The mobility monotonically decreases when the concentration of charge carriers increases. Figs. 2c and 2d show the dependence of the current density on the electric field at $n = 10^{12}\text{cm}^{-2}$, and for different temperatures. In obtaining these curves we have used that $J = nev$ and $neE = F_x$, where J and E are current density and electric field, respectively. Note that the current density saturate at $E \sim 0.5 - 2.0\text{V}/\ \mu\text{m}$, which is in agreement with experiment[27]. The saturation velocity can be extracted from the $I - E$ characteristics using $J_{sat} = nev_{sat}$, where 1.6 mA/μm is the saturated current density, and with the charge density concentration $n = 10^{12}\text{cm}^{-2}$: $v_{sat} \approx 10^6$m/s. Fig. 2c was calculated at $T_d = 0$ K. At zero temperature the van der Waals friction is due to quantum fluctuations of charge density, and is determined by the second term in Eq. (2)[9–12,28]

$$F_x(T_d = T_g = 0) = -\frac{\hbar}{\pi^3}\int_0^\infty dq_y \int_0^\infty dq_x \int_0^{q_x v} d\omega q_x e^{-2qd} \frac{\text{Im}R_d(\omega)\text{Im}R_g(\omega^-)}{|\ 1 - e^{-2qd}R_d(\omega)R_g(\omega^-)\ |^2} \tag{10}$$

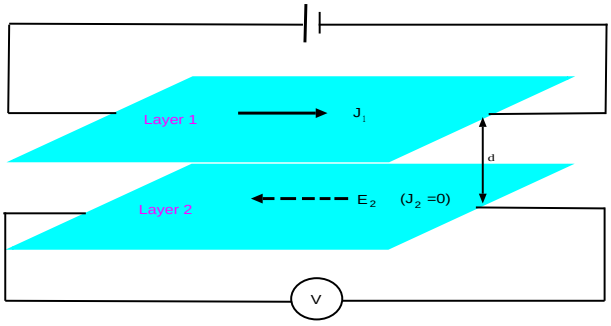

FIG. 3: A schematic diagram of a drag experiment. A current $\mathbf{J_1}$ is passed through layer **1**, and a voltmeter is attached to layer **2** to measure the induced electric field $\mathbf{E_2}$ due to the inter-layer interaction.

The existence of "quantum" friction is still debated in the literature[29–31]. The theory[9–12,28] predicts that a solid moving relative to another experiences a force due to quantum fluctuations, that is opposite to the direction of motion. The van der Waals friction can be studied in non-contact experiments, and in frictional drag experiments[10,11]. In both these experiments the solids are separated by a potential barrier thick enough to prevent electrons or other particle with a finite rest mass from tunneling across it, but allowing the interaction via the long-range electromagnetic field, which is always present in the gap between bodies. In non-contact friction experiments the damping of cantilever vibrations is typically measured, while in frictional drag experiments a current density is induced in one medium. The friction between the moving charge carriers and nearby medium gives rise to a change of $I-E$ characteristics, which can be measured.

The friction force acting on the charge carriers in graphene for high electric field is determined by the interaction with the optical phonons of the graphene, and with the optical phonons of the substrate. The frequency of optical phonons in graphene are a factor 4 larger than for the optical phonon in SiO_2. Thus, one can expect that for graphene on SiO_2 the high-field $I-E$ characteristics will be determined by excitations of optical phonons in SiO_2. According to the theory of the van der Waals friction[10,11], the "quantum" friction, which exist even at zero temperature, is determined by the creation of excitations in each of the interacting medium, the frequencies of which are connected by $vq_x = \omega_1+\omega_2$. The relevant excitations in graphene are the electron-hole pairs which frequencies begining from zero, while for SiO_2 the frequency of surface phonon polaritons $\omega_{ph} \approx 60$meV. The characteristic wave vector of graphene is determined by Fermi wave vector k_F. Thus the friction force is strongly enhanced when $v > v_{sat} = \omega_{ph}/k_F \sim 10^6$m/s, in the accordance with numerical calculations. Thus the measurements of the current density-electric field relation of graphene adsorbed on SiO_2 give the possibility to detect "quantum" friction, what has fundamental significance for physics.

An alternative method of studying of the van der Waals friction consists in driving an electric current in one metallic layer and studying of the effect of the frictional drag on the electrons in a second (parallel) metallic layer (Fig. 3). Such experiments were first suggested by Pogrebinskii[32] and Price[33], and were performed for 2D-quantum wells[34,35]. In these experiments, two quantum wells are separated by a dielectric layer thick enough to prevent electrons from tunneling across it, but allowing inter-layer interaction between them. A current density $J_1 = n_1 ev$ is driven through layer **1** (where n_1 is the carrier concentration per unit area in the first layer), see Fig. 3. Due to the inter-layer interactions a frictional stress $\sigma = \Gamma v$ will act on the electrons in layer **2** from layer **1**, which will induce a current in layer **2**. If layer **2** is an open circuit, an electric field E_2 will develop in the layer whose influence cancels the frictional stress σ between the layers. Experiments[34] show that, at least for small separations, the frictional drag can be explained by the interaction between the electrons in the different layers via the fluctuating Coulomb field. However, for large inter-layer separation the frictional drag is dominated by phonon exchange[36].

Similar to 2D-quantum wells in semiconductors, frictional drag experiments can be performed (even more easy) between graphene sheets. Such experiments can be performed in vacuum where the contribution from phonon exchange can be excluded. To exclude noise (due to presence of dielectric) the frictional drag experiments between quantum wells were performed at very low temperature ($T \approx 3$ K)[34]. For suspended graphene sheets there are no such problem and frictional drag experiment can be performed at room temperature. In addition, 2D-quantum wells in semiconductors have very low Fermi energy $\epsilon_F \approx 4.8\times 10^{-3}$eV[34]. Thus electrons in these quantum wells are degenerate only for very low temperatures $T < T_F = 57$ K. For graphene the Fermi energy $\epsilon_F = 0.11$eV at $n = 10^{12}$cm^{-2}, and the electron gas remains degenerate for $T < 1335$ K.

At small velocities the electric field induced by frictional drag depends linear on the velocity, $E = (\Gamma/ne)v = \mu^{-1}v$, where μ is the low-field mobility. For $\hbar\omega \ll \epsilon_F$ and $q \ll k_F$ the reflection amplitude for graphene is given by the same

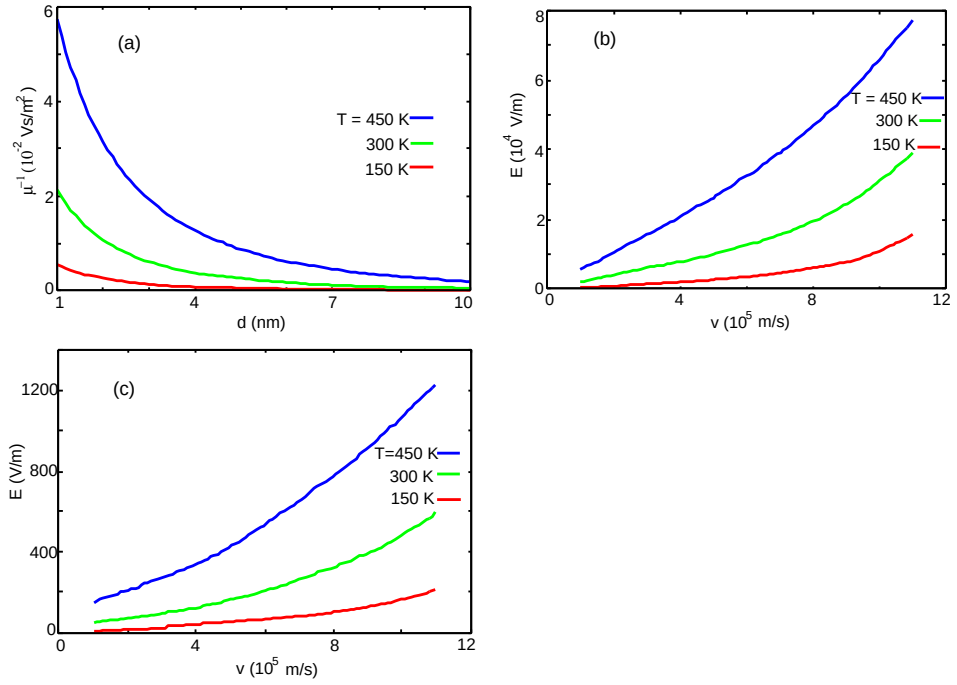

FIG. 4: Frictional drag between two graphene sheets at the carrier concentration $n = 10^{12}\text{cm}^{-2}$. (a) Dependence of friction coefficient per unit charge, $\mu^{-1} = \Gamma/ne$, on the separation between graphene sheets d. (b) Dependence of electric field induced in graphene on drift velocity of charge carriers in other graphene sheet at the layer separation $d = 1$ nm. (c) The same as in (b) but at $d = 10$nm.

expression as for a 2D-quantum well[10]:

$$R_g = 1 + \frac{\hbar\omega}{2k_F e^2} \tag{11}$$

Substitution of Eq. (11) into Eq. (8) gives

$$\Gamma = 0.01878\frac{\hbar}{d^4}\left(\frac{k_B T}{k_F e^2}\right)^2 \tag{12}$$

Fig. 4a shows the dependence of the friction coefficient (per unit charge) μ^{-1} on the separation d between the sheets. For example, $E = 5\times 10^{-4} v$ for $T = 300$ K and $d = 10$ nm. For a graphene sheet of length 1 μm, and with $v = 100$m/s this electric field will induce the voltage $V = 10$ nV. Figs. 5b and 5c shows the induced electric field-velocity relation for high velocity, with $d = 1$nm (b) and $d = 10$nm (c).

As discussed above, for graphene on SiO_2 the excess heat generated by the current is transferred to the substrate through the near-field radiative heat transfer, and via the direct phononic coupling (for which the thermal contact conductance $\alpha \approx 10^8 \text{Wm}^{-2}\text{K}^{-1}$). At small temperature difference ($\Delta T = T_g - T_d \ll T_d$), from Eq. (7) we get

$$\Delta T = \frac{F_{x0} v - S_{z0}}{\alpha_{ph} + S'_{z0} - F'_{x0} v} \tag{13}$$

where $F_{x0} = F_x(T_d, T_g = T_d)$, $S_{z0} = S_z(T_d, T_g = T_d)$,

$$F'_{x0} = \frac{dF_x(T_d, T_g)}{dT_g}\Big|_{T_g = T_d},\ S'_{z0} = \frac{dS_z(T_d, T_g)}{dT_g}\Big|_{T_g = T_d}$$

The thermal contact conductance is given by

$$\alpha = \frac{S_z(T_d, T_g) + \alpha_{ph}\Delta T}{\Delta T} \approx \frac{(\alpha_{ph} + S'_{z0})F_{x0} v - S_{z0} F'_{x0} v}{F_{x0} v - S_{z0}} \tag{14}$$

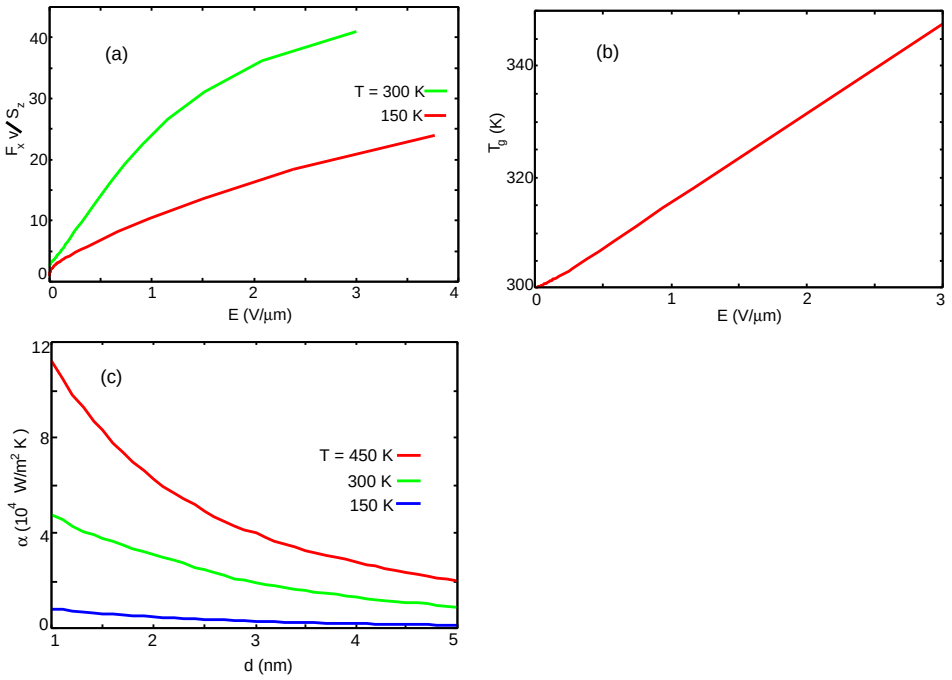

FIG. 5: Radiative heat transfer between graphene and SiO_2. (a) The dependence of the ratio between the total heat generated by current and the radiative heat flux, on electric field. $n = 10^{12}\text{cm}^{-2}$, $d = 3.5$Å, $\alpha_{ph} = 1.0 \times 10^8 \text{Wm}^{-2}\text{K}^{-1}$ (b) Dependence of graphene temperature T_g on the electric field. The substrate temperature $T_d = 300$ K. Parameters are the same as in (a). (c) Dependence of the thermal contact conductance on the separation d for low electric field, $\alpha_{ph} = 0$.

From Eq. (14) it follows that the thermal contact conductance can be strongly enhanced when $F_{x0}v \approx S_{z0}$. Fig. 5a shows the ratio of the total heat generated by the current to the radiative heat flux. For low field this ratio ~ 2 so that in this case both radiative heat transfer and phononic heat transfer give contributions of the same order. The phononic mechanism of heat transfer dominates for high electric field. For high electric field the equilibrium graphene temperature due to self-heating depends linear on the electric field (see Fig. 5b) in contrast to the low-field case where this dependence is quadratic. This can be explains by the fact that the saturation velocity depends weakly on electric field; therefore heat, generated by friction, will linearly depend on the electric field. Fig. 5c shows the dependence of the thermal contact conductance on the separation d for low electric field. At $d \sim 5$ nm and $T = 300$ K the thermal contact conductance, due to the near-field radiative heat transfer, is $\sim 10^4 \text{W}\cdot\text{m}^{-2}\cdot\text{K}^{-1}$, which is ~ 3 orders of magnitude larger than that of the black-body radiation. In comparison, the near-field radiative contact conductance in SiO_2-SiO_2 for the plate-plate configuration, when extracted from experimental data[20] for the plate-sphere configuration, is $\sim 2230 \text{W}\cdot\text{m}^{-2}\cdot\text{K}^{-1}$ at a $\sim$30 nm gap. For this system the thermal contact conductance depends on separation as $1/d^2$; thus $\alpha \sim 10^5 \text{W}\cdot\text{m}^{-2}\cdot\text{K}^{-1}$ at $d \sim 5$ nm what is one order of magnitude larger than for the graphene-SiO_2 system in the same configuration. However, the sphere has a characteristic roughness of ~ 40 nm, and the experiments[20,21] were restricted to separation wider than 30 nm (at smaller separation the imperfections affect the measured heat transfer). Thus the extreme near-field-separation, with d less than approximately 10 nm, may not be accessible using a plate-sphere geometry. On the other hand suspended graphene sheet has a roughness $\sim$1 nm[37], and measurements of the thermal conductance can be performed from separation larger than ~ 1 nm. At such separation one would expect the emergency of nonlocal and nonlinear effects. This range is of great interest for the design of nanoscale devices, as modern nanostructures are considerably smaller than 10 nm and are separated in some cases by only a few Angstroms. Another advantage of using graphene for studying the radiative heat transfer result from the fact that under steady-state condition the heat flow is equal to the heat generated in the graphene by the current density: $S_z = EJ$. This quantity can be accurately obtained from $I-V$ characteristics. The temperature of graphene can be measured accurately using Raman scattering spectroscopy[37].

Conclusion. We have used theories of the near-field radiative heat transfer and the van der Waals friction to study transport, heat generation and dissipation in graphene due to the interaction with phonon-polaritons in the (amorphous) SiO_2 substrate. In contrast with existing theories, based on the semiclassical Boltzmann transport equation, our approach is macroscopic. In the latter approach all microscopic properties are included in dielectric functions of material. Explicit formulas were obtained for the low-field mobility, the high-field transport and the

near-field radiative heat transfer between graphene and the substrate. The low-field mobility exhibit a strong temperature dependence, which (according to the theory of the van der Waals friction) is associated with the thermal fluctuation inside the media. High-field transport exhibit a weak temperature dependence, which can be considered as manifestation of quantum fluctuations. Thus the study of transport properties in graphene gives the possibility to detect "quantum" friction, the existence of which is still debated in literature. We have calculated the frictional drag between graphene sheets mediated by the van der Waals friction, and found that it can induce large enough voltage to be easily measured experimentally. This effect can be used in electronics and for sensoring. We have shown that for the low-field heat transfer between graphene and the substrate, both radiative heat transfer and phononic heat transfer give contributions of the same order. High-field heat transfer is determined by the phononic mechanism. We have pointed out that graphene can be used to study near-field radiative heat transfer in the plate-plate configuration, and for shorter separations than it is possible now in the plate-sphere configuration.

Acknowledgment

A.I.V acknowledges financial support from the Russian Foundation for Basic Research (Grant N 08-02-00141-a) and ESF within activity "New Trends and Applications of the Casimir Effect".

---

[1] Novoselov, K.S.; Geim, A.K.; Morosov, S.V.; Jiang, D.; Zhang, Y.; Dubonos, S.V.; Grigorieva, I.V.; Firsov, A.A. *Science* **2004**, *306*, 666-669.
[2] Novoselov, K.S.; Geim, A.K.; Morosov, S.V.; Katsnelson, M.I.; Grigorieva, I.V.; Dubonos, S.V.; Firsov, A.A. *Nature (London)* **2005**, *197*, 197-200.
[3] Geim, A.K.; Novoselov, K.S. *Nat. Mater.* **2007**, *6*, 183-191.
[4] Rytov, S. M. *Theory of Electrical Fluctuation and Thermal Radiation* (Academy of Science of USSR Publishing, Moscow, 1953)
[5] Levin, M. L.; Rytov, S. M. *Theory of eqilibrium thermal fluctuations in electrodynamics* (Science Publishing, Moscow, 1967)
[6] Rytov, S. M.; Kravtsov, Yu. A.; Tatarskii, V. I. *Principles of Statistical Radiophyics*(Springer, New York.1989), Vol.3
[7] E. M. Lifshitz *Zh. Eksp. Teor. Fiz.* **1955**,*29* , 94-110 [Sov. Phys.-*JETP* **1956**, *2*, 73-83]
[8] Polder, D.; Van Hove, M. *Phys. Rev. B* **1971**, *4*, 3303-3314
[9] Volokitin, A.I.; Persson,B.N.J. *J.Phys.: Condens. Matter* **11**, 345 (1999);*Phys.Low-Dim.Struct.***7/8**,17 (1998)
[10] Volokitin, A. I.; Persson, B. N. J. *Rev. Mod. Phys.* **2007**, *79*, 1291-1329
[11] Volokitin, A. I.; Persson, B. N. J. *Usp. Fiz. Nauk* **2007**, *177*, 921-951 [*Phys. Usp.* **2007**, **50**, 879-906
[12] Volokitin, A.I.; Persson, B.N.J. *Phys. Rev. B* **2008**, *78*, 155437.
[13] Volokitin, A.I.; Persson, B.N.J. *J.Phys.: Condens. Matter* **2001**, *13*, 859-873
[14] Volokitin, A.I.; Persson, B.N.J. *Phys. Rev. B* **2008**,*77*, 033413
[15] Rotkin, S.V.; Perebeinos, V.; Petrov, A.G.; Avouris, P. *Nano Lett.* **2009**, *9*, 1850-1855
[16] Perebeinos, V.; Avouris, P. *Phys. Rev. B* **2010**, *81*, 195442
[17] *Handbook of Nanoscience, Engineering and Technology*; Goddard, W., Brenner, D., Lishevski. S., Iafrate. G.J., Eds.; Taylor and Francis-CRC Press: Boca Raton, FL, 2007
[18] Persson, B.N.J.; Ueba, H. *Europhys. Lett.* **2010**, 91, 56001.
[19] Chen, D.Z.A.; Haman, R.; Soljacic, M.; Joannopoulos, J.D.; Chen, G. *Appl. Phys. Lett.* **2007**, 90, 181921
[20] Shen, S.; Narayanaswamy, A.; Chen, G. *Nano Lett.* **2009**, 9, 1883-1888.
[21] Rousseau, E.; Siria, A.; Jourdan, G.; Volz, S.; Comin, F.; Chevrier, J.; Greffet, J.J. *Nature Photon.* **2009**, *90*, 181921
[22] Joulain, K.;Mulet, J.P.;Marquier, F.;Carminati, R.; Greffet, J.J. *Surf. Sci. Rep.* **2005** , *57*,59-112
[23] Wunscvh, B.; Stauber, T.; Sols, F.; Guinea, F.; *New J.Phys.* **2006**, *8*, 318.
[24] Hwang, E.H.; Sarma, S.D.; *Phys. Rev. B* **2007**, *75*, 205418
[25] Chen, D.Z.A.; Hamam, R,; Soliači c, M.;Joannopoulos, J.D. *Appl. Phys. Lett.* **2007**, *90*, 181921
[26] Chen, J.H.; Jang, C.; Xiao, S.; Ishigami, M.; Fuhrer, M.S. *Nat. Nanotechnol.* **2008**, *3*, 206
[27] Freitag, M.; Steiner, M.; Martin, Y.; Perebeinos, V.; Chen, Z.; Tsang, J.C.; Avouris, P. *Nano lett.*, **2009**, *9*, 1883-1888
[28] Pendry, J.B. *J. Phys.C*, **1997**, *9*, 10301-10320
[29] Philbin, T.G.; Leonhardt, U. *New J. Phys.* **2009**, *11*, 033035
[30] Pendry, J.B. *New J. Phys.* **2010**, *12*, 033028
[31] Volokitin, A.I.; Persson, B.N.J. to be published
[32] Pogrebinskii, M.B. *Fiz.Tekh.Poluprov.* **1977**,*11*, 637-641 [*Sov.Phys. Semicond.* **1977**, *11*, 372-376].
[33] Price, P. J. *Physica B+C*, **1983**, *117*, 750-752
[34] Gramila, T.J.; Eisenstein, J.P.; MacDonald, A.H.; Pfeiffer, L.N.; West, K. W. *Phys. Rev. Lett.* **1991**, *66*, 1216-1219
[35] Sivan, U.; Solomon, P.M.; Shtrikman, H. *Phys. Rev. Lett.* **1992**, *68,* 1196-1199
[36] Bønsager, M.C.; Flensberg, K.; Hu, B. Y.K.; Macdonald, A.H. *Phys.Rev. B*, **1998**, *57*, 7085-7102
[37] Meyer, J.C.; Geim, A.K.; Katsnelson, M.I.; Novoselov, K.S.; Booth, T.J.; Roth, S. *Nature*, **2007**, *446*, 60-63